Stochastic Exposure Kinetics of EUV Photoresists: A Simulation Study

Chris A. Mack[a)], James W. Thackeray[b)], John J. Biafore[c)], Mark D. Smith[c)]

a) *Lithoguru.com, 1605 Watchhill Rd, Austin, TX 78703*
b) *Dow Advanced Materials, 455 Forest St., Marlborough, MA 01752*
c) *KLA-Tencor, FINLE Division, 8843 N. Capital of Texas Highway, Austin, TX 78759*

Abstract

BACKGROUND: The stochastic nature of extreme ultraviolet (EUV) resist exposure leads to variations in the resulting acid concentration, which leads to line-edge roughness (LER) of the resulting features.
METHODS: Using a stochastic resist simulator, we predicted the mean and standard deviation of the acid concentration for an open-frame exposure and fit the results to analytical expressions.
RESULTS: The EUV resist exposure mechanism of the PROLTIH Stochastic Resist Simulator is first order, and an analytical expression for the exposure rate constant *C* allows prediction of the mean acid concentration of an open-frame exposure to about 1% accuracy over a wide range of parameter values. A second analytical expression for the standard deviation of the acid concentration also matched the output of PROLITH to within about 1%.
CONCLUSIONS: Predicting the stochastic uncertainty in acid concentration for EUV resists allows optimization of resist processing and formulations, and may form the basis of a comprehensive LER model.

Keywords: Stochastic modeling, EUV photoresist, exposure kinetics, line-edge roughness, linewidth roughness, LER, LWR

I. INTRODUCTION

Unlike the direct photon absorption mechanism of exposure for 248-nm and 193-nm photoresists, Extreme Ultraviolet (EUV) resists are exposed via photo-ionization: a high-energy photon absorbed in the resist ionizes the polymer, generating an electron (called a photoelectron), which in turn can generate several secondary electrons.[1] These electrons then scatter through the resist losing energy and, occasionally, interacting with a photoacid generator (PAG) to generate an acid. Monte Carlo simulation of these events leads to a prediction of acid concentration as a function of exposure dose for a given set of resist parameters. Repeated simulations lead to prediction of both the mean and the standard deviation of the acid concentration. Both results are important in understanding EUV exposure kinetics and in predicting the impact of those kinetics on the line-edge and linewidth roughness of final lithographic images.

In this paper an exposure simulator using Monte Carlo, statistical-mechanical techniques called the PROLITH Stochastic Resist Model (version X3.2, from KLA-Tencor) is used to model both the mean and standard deviation of the acid concentration after exposure for the simple case of a large open-frame exposure. By finding the mean acid concentration as a function of exposure dose, the exposure rate constant for an EUV resist is extracted as a function of the stochastic resist parameters. A semi-empirical expression is developed that relates the value of this rate constant to the PROLITH resist parameters. Further, PROLITH simulations yield the standard deviation of the acid concentration, which is compared to a proposed theoretical expression. Based on these results, a comprehensive approach to reducing the relative uncertainty in the after-exposure acid concentration of an EUV resist is provided.

II. MEASURING C – A 193-NM RESIST TEST CASE

For a continuum lithography model, the exposure rate constant *C* is either a direct input to the model (one of the Dill ABC parameters[2]), or is easily calculated from other input parameters such as the molar

Extreme Ultraviolet (EUV) Lithography II, edited by Bruno M. La Fontaine, Patrick P. Naulleau, Proc. of SPIE
Vol. 7969, 796919 · © 2011 SPIE · CCC code: 0277-786X/11/$18 · doi: 10.1117/12.881066

absorptivity and quantum efficiency of the photoacid generator (PAG).[3] For a stochastic model, this is not necessarily the case. As we shall see below, the exposure model used by the PROLITH Stochastic Resist Model (SRM) for EUV resists does not have a first-order rate constant as an input, and in fact, it is not entirely clear that the exposure mechanism for an EUV resist will be first order. Thus, a method is needed for determining if a simulator's overall mechanism for generating acid from exposure is first order, and if so, what the exposure rate constant is.

Fortunately, a simple test case allows for developing and testing a method for extracting C from a stochastic simulator. For 193-nm resists, the exposure model in the PROLITH SRM is based on the standard photochemical mechanism of direct absorption of the photon by the PAG. This means that the relationship between the inputs to the SRM (the base-10 molar absorptivity (molar extinction coefficient) ε and the quantum efficiency ϕ) and the C parameter should hold, as long as the results are averaged over a large number of photon absorption events:

$$C = \phi \frac{2.303\,\varepsilon}{N_A}\left(\frac{\lambda}{hc}\right) \tag{1}$$

where h is Planck's constant, c is the vacuum speed of light, λ is the vacuum wavelength, and N_A is Avogadro's number.. Thus, after developing and applying the method for extracting C from the stochastic simulation output, we can compare the results to the calculated value of C from equation (1) to check the efficacy and accuracy of the method.

The PROLITH SRM has as an output the total number of acids generated during exposure in a preset simulation volume. Thus, the approach used here will be to simulate the exposure of an open frame and determine the number of acids generated as a function of exposure. To simplify the interpretation of the results, the resist, substrate, and immersion fluid will all be set to have the same refractive index as the resist so that no reflections will occur. This is not strictly possible in PROLITH since the immersion fluid must be non-absorbing (the imaginary part of its refractive index is fixed at 0), but the impact of this tiny mismatch in refractive index is entirely negligible (reflectivity = $\kappa^2/4 \approx 0.001\%$ for a typical resist, where κ is the imaginary part of the resist refractive index). To eliminate radiometric effects, the reduction ratio for the simulation is set to 1 and coherent illumination is used so that all light is normally incident on the resist. The grid size for all simulations is set to 1 nm. The remaining simulation parameters for this 193-nm test case are shown in Table I.

Table I: Stochastic resist parameters for 193-nm simulations

Exposure rate constant	0.024741 cm^2/mJ
Initial PAG density	0.05 /nm^3
Absorption coefficient α	0.0015 nm^{-1}
Open frame area	50 nm X 50 nm
Resist thickness	50 nm
Exposure dose range	1 – 100 mJ/cm^2
Exposure dose steps	1 mJ/cm^2
Number of trials per dose	100

For any given exposure dose, the number of acids generated in the volume of resist is calculated by the PROLITH SRM. An example output is shown in Figure 1. Since each data point is the output of a randomized (Monte Carlo) physical simulation of many photon absorption and exposure events, the size of

the resist volume has a large impact on the stochastic "noise" of the results. This stochastic uncertainty can be further averaged out by repeating simulations (called trials) at each dose. For most of the results presented here, 100 trials per dose were run and the average of the number of photoacids over the trials was used. This average number of photoacids (n_{acid}) is then converted into an average relative acid concentration (h_{AVG}) by

$$h_{AVG} = \frac{n_{acid}}{\rho_{PAG} V} \tag{2}$$

where ρ_{PAG} is the initial PAG density and V is the simulation volume.

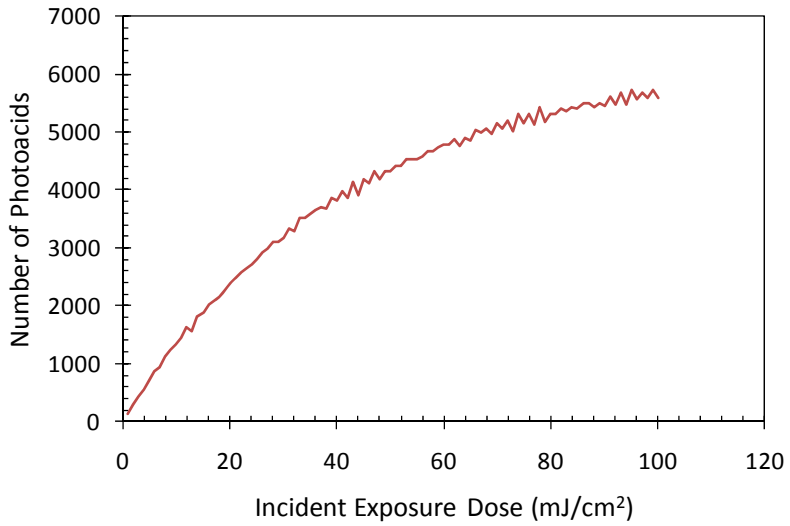

Figure 1. Monte Carlo simulation of the number of photoacids generated during 193-nm exposure of a 50X50X50 nm resist volume as a function of exposure dose.

For a first-order exposure mechanism, the relative acid concentration is related to the incident exposure dose E_i by

$$-\ln(1-h_{AVG}) \approx CE_{AVG} \tag{3}$$

where

$$E_{AVG} = \frac{1}{D}\int_0^D E_i e^{-\alpha z} dz = E_i\left(\frac{1-e^{-\alpha D}}{\alpha D}\right) \tag{4}$$

and α is the resist absorption coefficient and D is the resist thickness. The derivation of these expressions are given in the Appendix. The linear relationship in equation (3) is only approximate due to the non-linear affect of absorption through the thickness of the resist. However, for a thin enough resist this linear approximation is a good one (see the Appendix for more details), and so will be used throughout this paper.

Figure 2 shows an example simulation for the 193-nm resist test case with 100 trials per exposure dose. The input values of PAG molar absorptivity and quantum efficiency give a value of C of 0.024741 cm^2/mJ and, in this simulation, the extracted slope was 0.024736 cm^2/mJ with a standard error of the slope equal to 1.0 X 10^{-5} cm^2/mJ (0.041%). Repeating this simulation experiment 20 times, the mean value of C was 0.0247381 cm^2/mJ with a standard deviation of 1.1 X 10^{-5} cm^2/mJ (0.045%), and a standard error of the mean equal to 2.5 X 10^{-6} cm^2/mJ (0.014%). The standard error of the slope is approximately equal to the standard deviation of the extracted value of C, with no statistically significant deviation from the true value of C. Thus, given the caveats discussed in the Appendix, this method provides a reliable value for the first-order exposure rate constant C from Monte Carlo simulations of exposure.

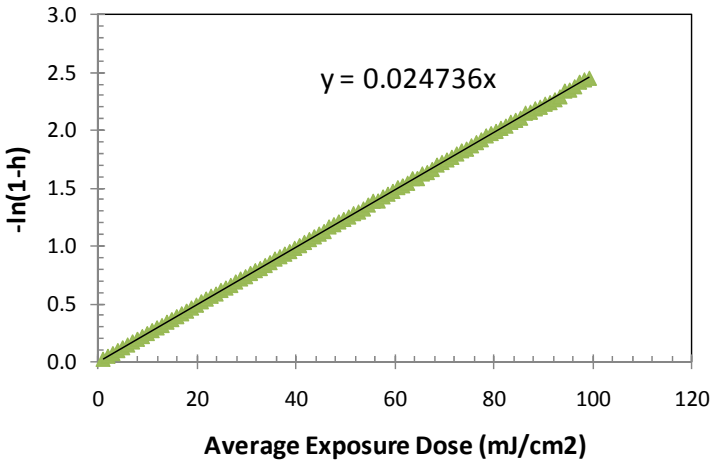

Figure 2. Measurement of the exposure rate constant C as the slope of the line in this plot (data generated by the PROLITH SRM for a 193-nm resist).

III. MEASURING C – STOCHASTIC EUV RESIST MODEL

The stochastic EUV resist model of the PROLITH SRM does not assume a first-order exposure model *per-se*, but instead simulates a sequence of more elementary steps that lead to the generation of an acid.[4] Photons originating from the projection optics impinge upon the resist film. The number of photons absorbed by the resist is determined by Lambert's law and Poisson statistics (in this study, the PAG is assumed to not directly absorb photons). Once a photon has been absorbed, one electron is (possibly) released with probability ϕ_e, and with kinetic energy equal to the photon energy minus the ionization potential, IP. This photoelectron (or primary electron) then travels and scatters through the resist, possibly inducing further ionization and resulting in a secondary electron cascade. The interaction of scattering electrons with the resist involves (at least) elastic and inelastic collisions: in an elastic collision the resist is left in the original state; in an inelastic collision the resist is ionized and a secondary electron ejected. As they travel through the resist, electrons lose kinetic energy continuously (in a *continuous slowing-down approximation*). The stopping power of the resist is the energy lost by an electron per path length traveled and is calculated with the complex dielectric function for a model compound (polystyrene, C_8H_8). Photoacid generators are randomly dispersed throughout the resist with average density ρ_{PAG}. Electrons traveling within the reaction radii (r) of PAGs may be of energy sufficient to produce excitation (PAG Excitation Energy, E_{excit}). PAGs in an electronically-excited state are converted to acid with a probability given by the PAG quantum efficiency (ϕ_{PAG}). Further details of this exposure model have been previously published.[4]

Thus, there are a large number of parameters that influence the generation of an acid or acids for any given EUV photon incident on the resist. The baseline values of these parameters for the simulations in this paper are given in Table II. As various parameter values were changed in the studies presented below, the exposure dose range was adjusted so that at the highest dose approximately 90% of the PAG was converted to acid.

Table II: Stochastic resist parameters for EUV simulations

PAG Molar Absorptivity	0
Initial PAG Density, ρ_{PAG}	0.05 /nm^3
Absorption Coefficient, α	0.006516 nm^{-1}
Electron Generation Efficiency, ϕ_e	0.9
Ionization Potential, *IP*	10 eV
PAG Excitation Radius, *r*	2.0 nm
PAG Excitation Energy, E_{excit}	5 eV
PAG Quantum Efficiency, ϕ_{PAG}	0.5
Open frame area	50 nm X 50 nm
Resist thickness	10 nm
Exposure dose range	0.25 – 25 mJ/cm^2
Exposure dose steps	0.25 mJ/cm^2
Number of trials per dose	100

In all of the studies presented below, the EUV stochastic resist model of PROLITH exhibited overall first-order exposure kinetics, so that the method for extracting *C* described in the previous section could be applied. With 100 trials per exposure dose, the 95% confidence interval for a typical value of *C* is about ±0.07%. Each of the parameters of the model were varied in order to understand their impact on *C*. As expected, PAG density did not affect the value of *C*. Other parameters were more interesting.

a. Absorption Coefficient

Since only an absorbed photon can generate photo- and secondary electrons and cause acid generation, one would expect a monotonic increase in *C* with absorption coefficient. The Lambert law of absorption essential says that the absorption probability per unit length traveled is a constant, equal to the absorption coefficient of the material α. Since the model used here assumes that all absorption is done by the polymer, each absorption event is equally likely to result in a photoelectron. Thus, one expects to find that *C* is proportional to α. Figure 3 confirms this expectation. Since the resist thickness was fixed a 10 nm, a high absorption coefficient (> 0.01 nm^{-1}) produces a non-linear effect through the resist thickness, as discussed in the Appendix.

b. Electron Generation Efficiency

Given the model used here, one would expect that *C* would be directly proportional to the electron generation efficiency, ϕ_e. Simulation results confirm this prediction, as seen in Figure 4.

c. Ionization Potential

When photon absorption leads to the generation of a photoelectron, the resulting electron has initial kinetic energy equal to the photon energy minus the ionization potential, *IP*. Thus, higher ionization

potential leads to a lower energy electron, which then has less energy available to find a PAG and cause photoacid generation. Simulations show that the impact of ionization potential can be well described by

$$C = C_0\left(1 - \frac{IP}{IP_0}\right) \tag{5}$$

where C_0 is the value of C when $IP = 0$, and IP_0 is the value of the ionization potential that makes $C = 0$. Thus, one expects IP_0 to about equal to the photon energy (91.8 eV for an EUV photon) minus the PAG excitation energy. Figure 5 shows that equation (5) does fit the simulated results, but with the value of IP_0 dependent upon the mechanism for PAG reaction with the secondary electron. For these simulations, IP_0 = 103 eV when the PAG reaction radius r = 1 nm, and IP_0 = 111 eV when r = 2 nm.

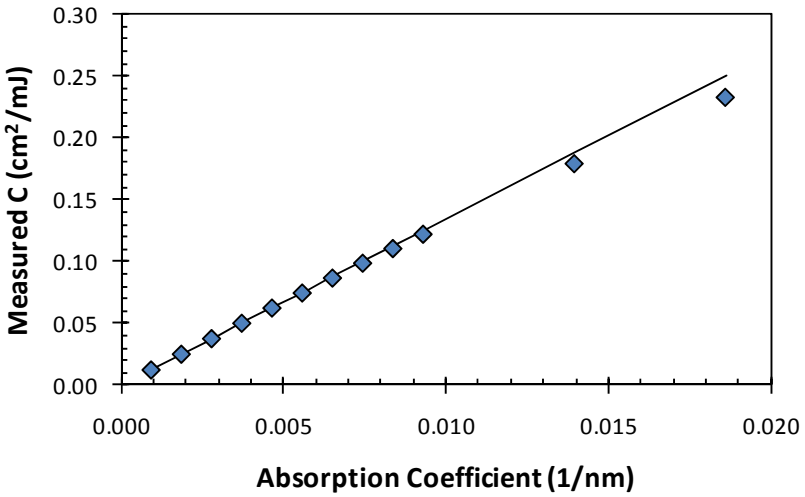

Figure 3. Measurement of the EUV resist exposure rate constant *C* as a function of the resist absorption coefficient α.

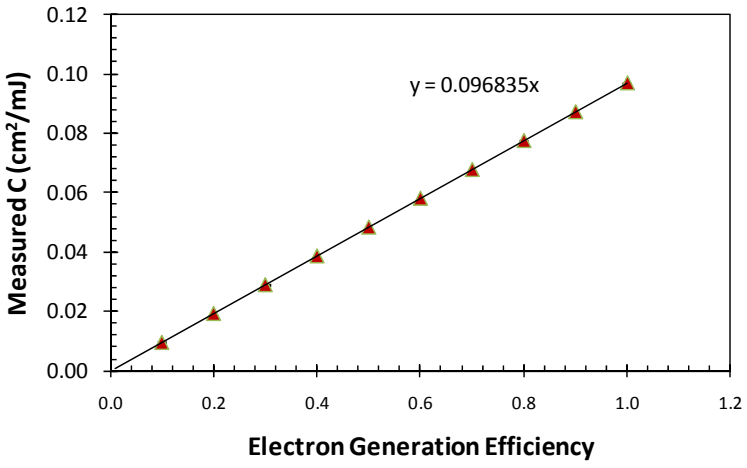

Figure 4. Measurement of the EUV resist exposure rate constant *C* as a function of the electron generation efficiency ϕ_e.

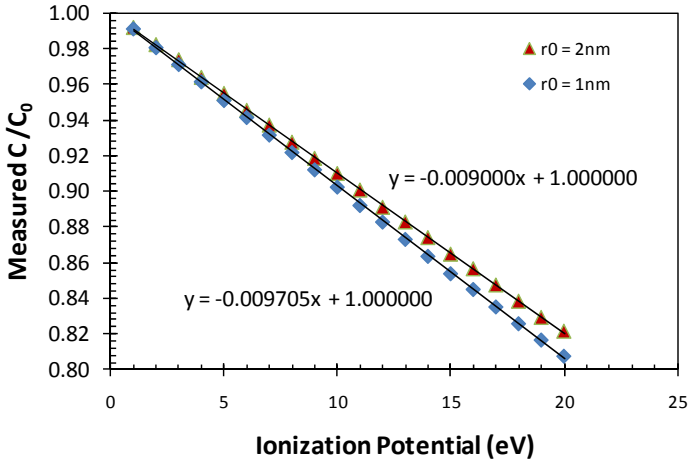

Figure 5. Measurement of the EUV resist exposure rate constant *C* as a function of the ionization potential *IP* for two different values of the PAG reaction radius, *r*.

The value of IP_0 extracted from these simulations as a function the PAG reaction radius (with the PAG excitation energy fixed at 0.2 or 5 eV) is shown in Figure 6. Using the PAG reaction cross-section ($\sigma_{e\text{-}PAG}$, with units of nm^2) defined in the following sections, Figure 6b shows that IP_0 matches the expected value (91.8 eV – E_{excit}) when the reaction cross-section goes to zero, and follows this empirical expression in general:

$$IP_0 = 91.8eV - E_{excit} + 16.4\left(\sigma_{e-PAG}\right)^{0.15} \tag{6}$$

While equation (6) matches the simulated results quite well, the simpler approach of fixing the value of IP_0 to about 110 eV in equation (5) provides a reasonable estimation of the impact of ionization potential on *C* for a reasonable range of PAG reaction parameters.

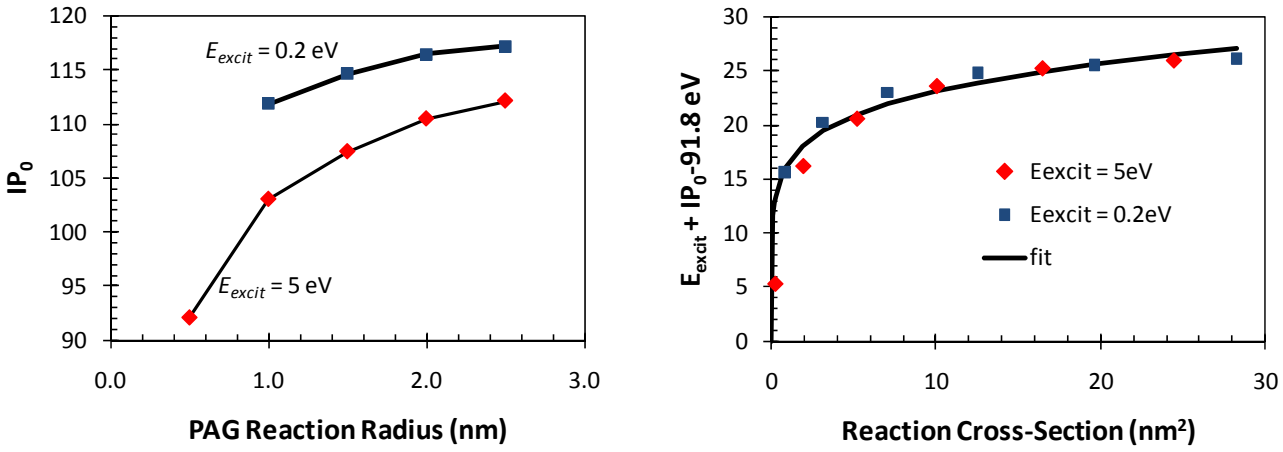

Figure 6. a) The extracted value of IP_0 as a function of the PAG reaction radius, *r*, for two different PAG excitation energies. b) as a function of the PAG reaction cross-section.

d. PAG Reaction Radius

When an electron comes within the PAG reaction radius, r, of a (randomly positioned) PAG molecule, a reaction is possible. Thus, a larger PAG reaction radius is expected to yield a larger value of C. This concept, in fact, is the same as that of a reaction cross-section, where the reaction rate is proportional to the reaction cross-section, which in turn is proportional to the reaction radius squared. The continuous slowing down approximation assumes that the traveling electron is losing energy per nanometer traveled to its environment. When the electron is within the reaction radius, the energy lost by the electron is transferred to the PAG. Only if the energy lost to the PAG is greater than the PAG excitation energy will there be a chance of generating an acid. This means there will be a minimum PAG reaction radius for reaction (r_0), below which even the most energetic electron will not be able to transfer enough of its energy to the PAG in order to overcome this excitation barrier. Thus, an expected behavior is

$$C \propto \sigma_{e-PAG}, \quad \sigma_{e-PAG} = \pi(r - r_0)^2 \tag{7}$$

where $\sigma_{e\text{-}PAG}$ is the electron-PAG reaction cross-section.

Figure 7 shows the PROLITH simulation results for C as a function of PAG reaction radius, for two different PAG excitation energies (2.2 and 5.0 eV). The quadratic model fits the data very well, with r_0 a function of the PAG excitation energy (as will be discussed in the following section).

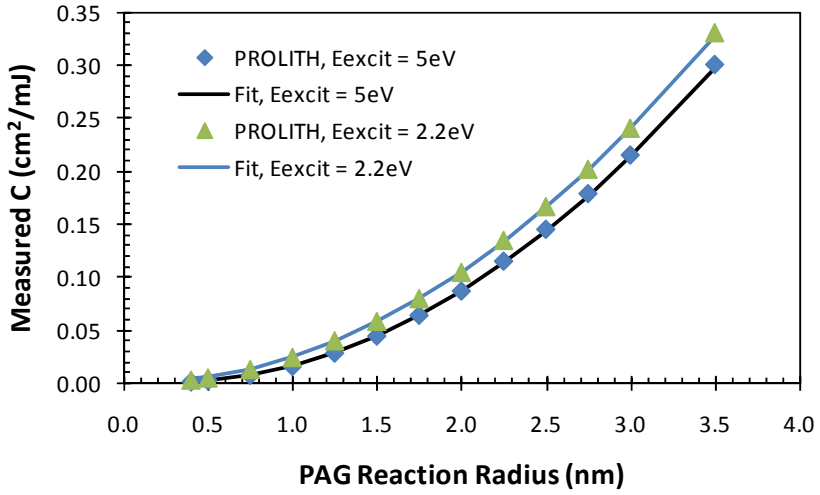

Figure 7. Measurement of the EUV resist exposure rate constant C as a function of the PAG reaction radius for two different values of the PAG excitation energy, E_{excit}. Fit curves follow equation (7).

e. PAG Excitation Energy

When energy is transferred from a secondary electron to a PAG molecule, the generation of an acid is possible only if the energy transferred exceeds a threshold value, called the PAG excitation energy, E_{excit}. As mentioned in the preceding section, simulations have shown that the impact of changing E_{excit} can be modeled as simply a change in the value of r_0. Figure 8a shows the simulation results for two different PAG

reaction radii. For moderately low excitation energies (less than or equal to about 5 eV), the fall-off is approximately quadratic. In fact, data in this range of excitation energies can be well fit by

$$r_0 = 0.0084 E_{excit}^2 \tag{8}$$

(where r_0 is in nanometers and E_{excit} is in electron-volts). For higher excitation energies, a more complex model will be required (see Figure 8b).

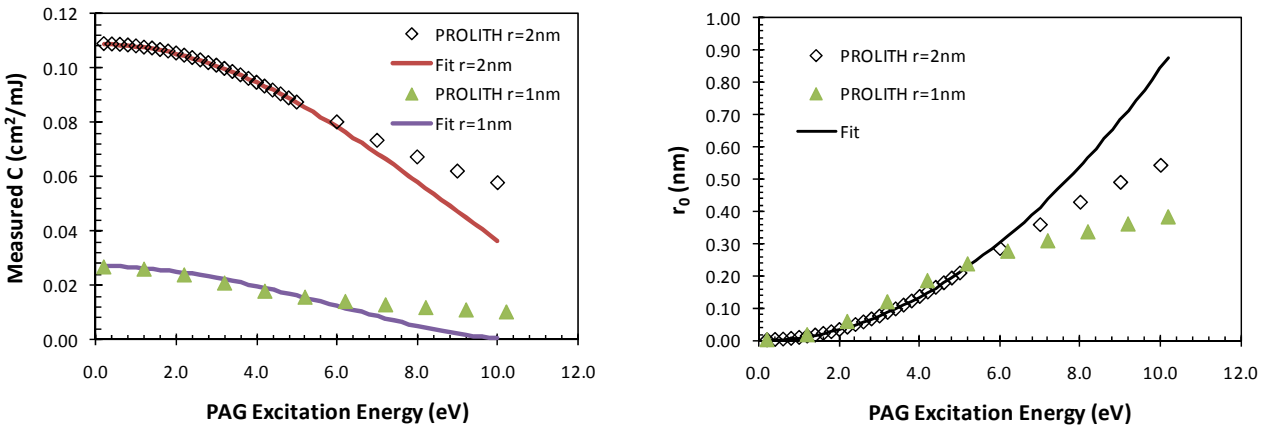

(a) (b)

Figure 8. Measurement of the EUV resist exposure rate constant *C* as a function of the PAG excitation energy for two different values of the PAG reaction radius, *r*. For both graphs, the fit curves follow equations (7) and (8).

f. PAG Quantum Efficiency

When a PAG molecule receives energy in excess of the required excitation energy, an acid is generated with probability equal to the PAG quantum efficiency, ϕ_{PAG}. At first thought, one would expect C to be linearly proportional to ϕ_{PAG}. Simulations (as given in Figure 9) show a more interesting behavior. As the quantum efficiency approaches 1, the impact on C begins to saturate: there is a smaller incremental increase in C for the same incremental increase in ϕ_{PAG}. Further reflection, however, makes the reason for this behavior clear.

One of the most interesting aspects of an EUV resist is the possibility of an acid yield (the average number of generated acids per absorbed photon) greater than 1. Since the energy of one EUV photon (92 eV) far exceeds the minimum energy required to convert a PAG into an acid (on the order of 5 eV), each absorbed photon can potentially generate many acids. But for that to happen, there must be a sufficient number of unreacted PAGs in the neighborhood of the absorption event. Consider the initial (low-dose) acid yield, Y_0, defined as

$$Y_0 = \lim_{dose \to 0} \left(\frac{\#acids}{\#absorbed\ photons} \right) \tag{9}$$

From the definition of C, this initial acid yield will be

$$Y_0 = \frac{C}{\alpha}\left(\frac{hc}{\lambda}\right)\rho_{PAG} \tag{10}$$

As the density of unreacted PAGs decreases with higher exposure doses, the acid yield must also decrease, leading to a saturation in how large *C* can be.

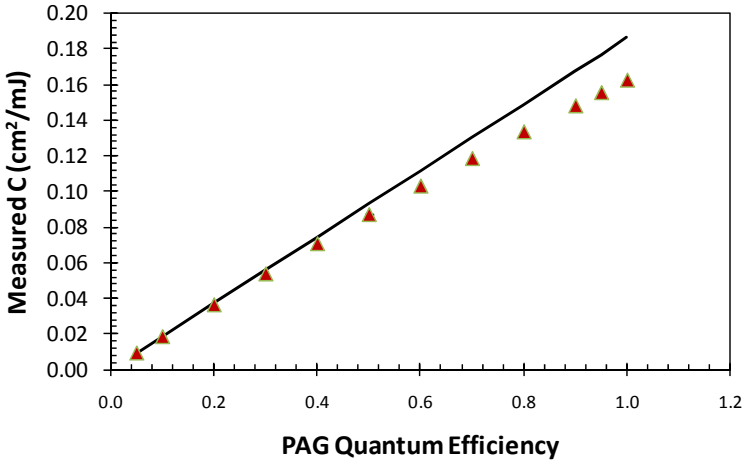

Figure 9. Measurement of the EUV resist exposure rate constant *C* as a function of the PAG quantum efficiency. A straight line through the first few data points is shown for comparison.

To quantify this saturation, let r_e be the maximum distance a secondary electron can travel from the point of photon absorption and still have sufficient energy to excite a PAG. The maximum number of PAGs that can possibly be converted by one absorbed photon is then the number of PAGs to be found in a sphere of this radius:

$$Max\,\#\,acids = \left(\frac{4}{3}\pi r_e^3\right)\rho_{PAG} \tag{11}$$

The maximum possible acid yield occurs when this number of acids are generated for each absorbed photon. This leads, then, to a maximum possible value of *C*, called $C_{\max}$:

$$C_{\max} = \left(\frac{4}{3}\pi r_e^3\right)\alpha\left(\frac{\lambda}{hc}\right) \tag{12}$$

Note that the maximum possible value of *C* does not depend on the initial PAG density. It depends entirely on the absorption coefficient and r_e, the maximum distance a secondary electron can travel and still have sufficient energy to excite a PAG. The existence of $C_{\max}$ leads to the observed saturation of *C* as the PAG quantum efficiency grows. The observed nonlinear behavior seen in Figure 9 can now be fit with a semi-empirical expression for this saturation:

$$C = C_{\max}\left(1 - e^{-\gamma\phi_{PAG}}\right) \tag{13}$$

where γ determines the degree of nonlinearity. Fitting equation (13) to the simulated data of C vs. ϕ_{PAG} allows both γ and $C_{\max}$ (and thus r_e) to be determined. Table III shows the results of such a fit for several sets of model input parameters. It is very interesting that this approach provides not only a model for the behavior of C with ϕ_{PAG}, but a way of extracting the "electron blur" of the model, the effective distance that photo- and secondary electrons travel while causing acid generation. For the range of model parameters investigated here, this electron blur radius is in the range of 2.1 to 3.3 nm.

Table III: Impact of various model parameters on the saturation of the exposure rate constant

Ionization Potential (eV)	PAG Excitation Energy (eV)	PAG Reaction Radius (nm)	$C_{\max}$ (cm^2/mJ)	r_e (nm)	Nonlinear Term γ
10	5	2	0.65	3.3	0.29
0.1	5	2	0.61	3.2	0.34
10	0.2	2	0.58	3.1	0.41
10	5	1	0.17	2.1	0.20

g. Overall Model for C

Combining all of the observations described above, an analytical model for C based on the PROLITH EUV SRM can be established. For the case where the PAG excitation energy is about 5 eV or less, and the PAG quantum efficiency is low enough that the nonlinear saturation of equation (13) can be ignored,

$$C \approx d_0\left(1-\frac{IP}{110eV}\right)\alpha\phi_e\phi_{PAG}\,\sigma_{e-PAG}\left(\frac{\lambda}{hc}\right) \tag{14}$$

where $\sigma_{e-PAG}=\pi\left(r-r_0\right)^2$ and $r_0=0.0084E_{excit}^2$, and where the constant d_0 is empirically determined to be 4.75 nm. [It is interesting to note that equation (14) is based on the results of well over one million open-frame stochastic exposure simulations.] Over a useful range of model input parameters, this semi-empirical expression predicts the value of C obtained from the PROLITH Stochastic Resist Model version X3.2 to within about 1–2%. More complicated expressions are certainly possible if PAG excitation energies greater than 5 eV or PAG quantum efficiencies near 1 are to be used, or if a more accurate model for the impact of ionization potential is desired. It would also be interesting to discover what details of the electron scattering and energy loss model give rise to the specific values of the empirical constants observed here.

h. Theoretical Model for C

Equation (14) is a semi-empirical model that replicates the mean outcome of the PROLITH SRM with reasonable accuracy. Here, a simplified two-step mechanism for EUV exposure will lead to an analytical rate equation that can be compared this semi-empirical result. Consider first the generation of photoelectrons. Letting ρ_{pe} be the number density of photoelectrons generated by exposure, a standard kinetic rate equation for photoelectron generation will be similar to the standard rate equation for direct photon resist exposure:[5]

$$\frac{d\rho_{pe}}{dt}=\alpha\phi_e I\left(\frac{\lambda}{hc}\right) \tag{15}$$

where I is the intensity of light. Solving this rate equation,

$$\rho_{pe} = \alpha \phi_e E \left(\frac{\lambda}{hc} \right) \tag{16}$$

where E is the exposure dose.

Now, let these photoelectrons migrate through the resist, colliding with a PAG to generate an acid. A standard second-order rate equation based on collision kinetic theory would look like

$$\frac{d\rho_{PAG}}{dt} = v \phi_{PAG} \sigma_{e-PAG} \rho_{pe} \rho_{PAG} \tag{17}$$

where $\sigma_{e\text{-}PAG}$ is the reaction cross-section between the electron and the PAG and v is the velocity of the electron. Note that t in this equation is the time the electron spends moving about the resist and reacting with PAGs. Combining equations (16) and (17) and integrating,

$$\rho_{PAG} = \rho_{PAG-0} e^{-K}, \text{ where } \quad K = v \phi_{PAG} \sigma_{e-PAG} \int_0^\infty \rho_{pe} dt \tag{18}$$

Defining the lifetime τ of the photoelectron as

$$\tau = \frac{1}{\rho_{pe}(t=0)} \int_0^\infty \rho_{pe} dt \tag{19}$$

and noting that the photoelectron density at $t = 0$ is given by equation (16), we have

$$K = CE = \alpha \phi_e \phi_{PAG} \sigma_{e-PAG} E \left(\frac{\lambda}{hc} \right) v \tau \tag{20}$$

Letting $d_e = v\tau$, this quantity can be thought of as the mean effective path length of the photoelectron traveling in the resist. If the photoelectron generates secondary electrons, then this distance can be interpreted as the mean sum of the path lengths of all the electrons. The final result is

$$C = d_e \phi_e \alpha \phi_{PAG} \sigma_{e-PAG} \left(\frac{\lambda}{hc} \right) \tag{21}$$

Comparing this theoretical expression for the overall exposure rate constant to the equation (14) fit to the results of PROLITH SRM simulations, we see that they are identical when

$$d_e = d_0 \left(1 - \frac{IP}{110eV} \right) \tag{22}$$

The empirically derived value of 4.75 nm for d_0 can now be interpreted as the mean electron path length in the resist for the limiting case of $IP = 0$.

Thus, the simplified two-step kinetic exposure model presented in this section matches the overall results obtained from the more detailed mechanism embedded in the PROLITH SRM. Of course, the more detailed EUV exposure mechanism in PROLITH allows d_e and $\sigma_{e\text{-}PAG}$ to be expressed as a function of more fundamental scattering and reaction parameters. Note also that a simplified mechanism where only one photoelectron reacts with PAGs does not alter the overall form the expression for C compared to the case where a cascade of secondary electrons can react with the PAGs.

IV. EUV ACID FLUCTUATIONS

The previous section described an analytical model that could predict the average number of acids generated in a given volume as a function of exposure dose. From the perspective of line-edge roughness (LER), a more important term to predict is the standard deviation of the acid concentration. By simulating open frame exposures with the PROLITH SRM, this standard deviation can also be extracted.

For a 193-nm resist, the exposure mechanism is simple enough that an analytical expression for the standard deviation of the acid concentration can be derived.[6,7] Defining $\langle h \rangle$ as the mean concentration of acid relative to the initial concentration of unexposed PAG [essentially the same as h_{AVG} from equation (2)], the standard deviation of this acid concentration in some volume V will be σ_h, given by

$$\left(\frac{\sigma_h}{\langle h \rangle}\right)^2 = \frac{1}{\langle h \rangle \langle n_{0-PAG} \rangle} + \left(\frac{\left(1-\langle h \rangle\right)\ln\left(1-\langle h \rangle\right)}{\langle h \rangle}\right)^2 \frac{1}{\langle n_{0-PAG} \rangle \langle n_{photons} \rangle} \tag{23}$$

where $\langle n_{0-PAG} \rangle = \rho_{PAG} V$ is the mean number of PAGs initially found in that volume and $\langle n_{photons} \rangle$ is the mean number of photons incident upon the top of the resist volume. This result is reasonably intuitive. The first term on the right-hand side of equation (23) is the expected Poisson result based on exposure kinetics – the relative uncertainty in the resulting acid concentration after exposure goes as one over the square root of the mean number of acid molecules generated within the volume of interest. For large volumes and reasonably large exposure doses, the number of acid molecules generated is large and the statistical uncertainty in the acid concentration becomes relatively small. For small volumes or low doses, a small number of photogenerated acid molecules results in a large relative uncertainty in the actual number within that volume. The second term accounts for photon shot noise and adds to the variance due to chemical concentration shot noise (making the final uncertainty worse than Poisson). For 193-nm resists, the impact of this photon shot noise term is minimal compared to variance in acid concentration caused by simple molecular position uncertainty. Unfortunately, the same is not true for EUV resists.

The second term on the right side of equation (23) includes the product of the number of photons and the number of PAGs, the absorbing species. This product is an obvious consequence of the mechanism of exposure for 193-nm resists. For EUV resists, however, the entire resist is an absorption site, so that stochastic uncertainty is not limited by photons finding an appropriate absorption site. Instead, the stochastic limiter is the number of photoelectrons generated. Thus, by analogy with the result for 193-nm resists, an expected behavior for EUV resists would be

$$\left(\frac{\sigma_h}{\langle h\rangle}\right)^2 = \frac{1}{\langle h\rangle\langle n_{0-PAG}\rangle} + \left(\frac{(1-\langle h\rangle)\ln(1-\langle h\rangle)}{\langle h\rangle}\right)^2 \frac{1}{\langle n_{photoelectrons}\rangle} \tag{24}$$

where $\langle n_{photoelectrons}\rangle = \phi_e \langle n_{photons}\rangle (1-e^{-\alpha D}), \quad \langle h\rangle = e^{-C\langle E_{AVG}\rangle}$

and $\langle n_{photoelectrons}\rangle$ is the mean number of photoelectrons generated in the volume. It is expected that this equation can be derived directly from the simplified two-step exposure mechanism described in the previous section.

To test this hypothesis, the PROLITH SRM was run over a range of parameters using the same open-frame exposure approach as described above for determining *C*. For each open-frame simulation, the number of acids found in the volume at the end of exposure is determined. Repeating the simulation many (typically 4,000 – 20,000) times, both the mean number of acids and the standard deviation are calculated. To get the best match to the simulated data (with residuals whose mean is near zero and with minimum variance), a slight modification to equation (24) was required:

$$\left(\frac{\sigma_h}{\langle h\rangle}\right)^2 = \frac{1}{\langle h\rangle\langle n_{0-PAG}\rangle} + 1.07\left(\frac{(1-\langle h\rangle)\ln(1-\langle h\rangle)}{\langle h\rangle}\right)^2 \frac{1}{\langle n_{photoelectrons}\rangle} \tag{25}$$

The reason why the second term on the right hand side of equation (25) had to increase by 7% in order to match the PROLITH SRM output is not clear. A typical result, using the nominal parameters of Table II, is shown in Figure 10. The fit of this equation to the PROLITH SRM data is remarkably good.

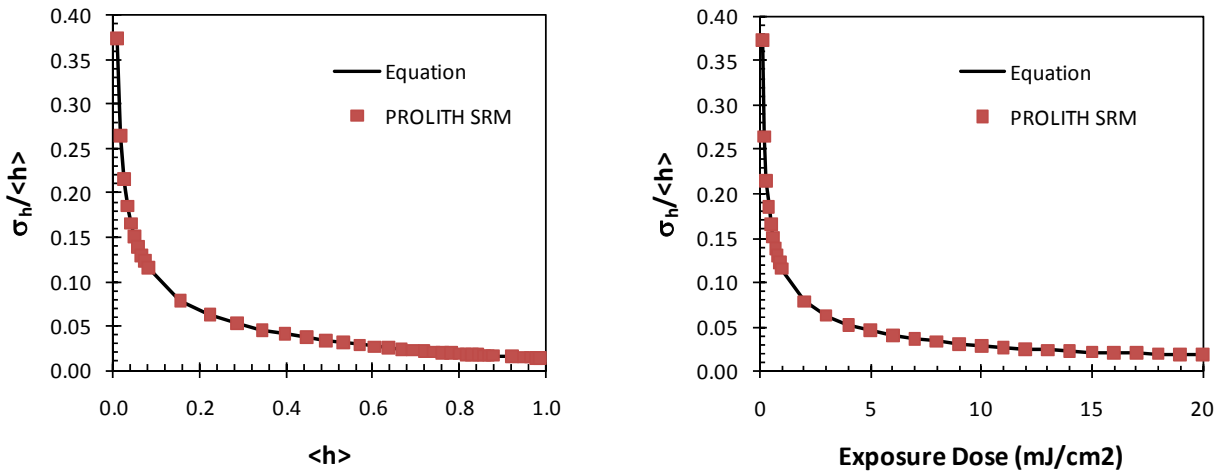

(a) (b)

Figure 10. Typical example (using the baseline parameters of Table II, with *C* = 0.08652 cm^2/mJ) of how the relative uncertainty in acid concentration varies with (a) the mean acid concentration, and (b) the incident exposure dose. Symbols give the PROLITH SRM simulation results, the solid line shows the prediction of equation (25).

To test the accuracy of equation (25), all of the EUV exposure model parameters were varied to determine their impact on the variance of the acid concentration. For the nominal case of Figure 10, the RMS error between PROLITH and the analytical expression is less than 0.5% over the range of exposure doses used. In Figure 11 the PAG quantum efficiency was varied (with the impact of changing C). The analytical model of equation (25) matches the PROLITH SRM results extremely well for ϕ_{PAG} = 0.25, 0.5 and 1.0 (RMS errors between 1 and 2%). Further tests set the imaginary part of the resist refractive index κ to 0.004, 0.007, and 0.01; the photoelectron generation probability ϕ_e to 0.45 and 0.9; the ionization potential IP to 1 eV, 10 eV, and 20 eV; the PAG reaction radius r to 1 nm, 2 nm, and 3nm; and the PAG excitation energy to 2 eV and 5 eV. In all cases, the analytical model of equation (25) matches the PROLITH SRM results with this same level of accuracy (typical RMS errors near 1%). Figure 12 shows the impact of varying the initial PAG density ρ_{PAG}, with values of 0.1, 0.2, and 0.4 nm^{-3}. Again, equation (25) matches the PROLITH SRM results extremely well (RMS errors below 1%).

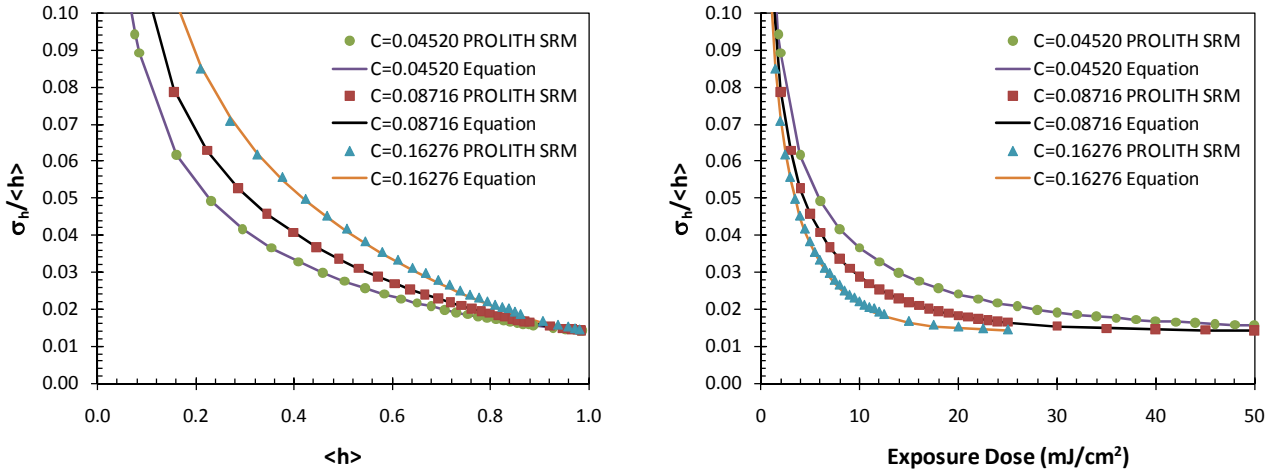

Figure 11. Impact of PAG quantum efficiency (with values of 0.25, 0.5, and 1.0) on the relative uncertainty in acid concentration, shown as a function of mean relative acid concentration and of dose. Symbols give PROLITH SRM results, the solid lines show the prediction of equation (25).

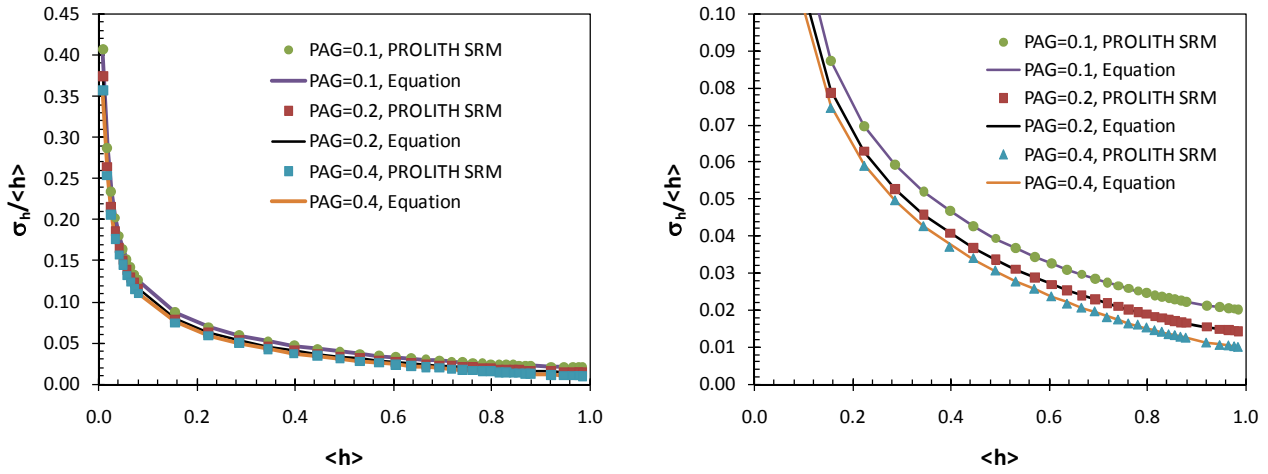

Figure 12. Impact of initial PAG loading (with values of 0.1, 0.2, and 0.4 nm^{-3}) on the relative uncertainty in acid concentration. Symbols give the PROLITH SRM simulation results, the solid lines show the prediction of equation (25). The two figures differ only in the scale of the y-axis.

An interesting simplification to equation (23) comes for the case of αD « 1.

$$\left\langle n_{photoelectrons} \right\rangle \approx \alpha D \phi_e \left\langle n_{photons} \right\rangle = \alpha \phi_e E \left(\frac{\lambda}{hc} \right) V \tag{26}$$

so that the ratio of the mean initial number of PAGs to the mean number of photoelectrons is

$$\frac{\left\langle n_{0-PAG} \right\rangle}{\left\langle n_{photoelectrons} \right\rangle} \approx \frac{\rho_{PAG}}{\alpha \phi_e E \left(\frac{\lambda}{hc} \right)} = \left[\frac{C \left(\frac{hc}{\lambda} \right)}{\alpha \phi_e} \right] \left[\frac{\rho_{PAG}}{-\ln\left(1 - \left\langle h \right\rangle\right)} \right] \tag{27}$$

Recalling the definition of initial acid yield from equation (10),

$$\frac{\left\langle n_{0-PAG} \right\rangle}{\left\langle n_{photoelectrons} \right\rangle} \approx \frac{-1}{\ln\left(1 - \left\langle h \right\rangle\right)} \frac{Y_0}{\phi_e} \tag{28}$$

Thus, equation (23) becomes

$$\left(\frac{\sigma_h}{\left\langle h \right\rangle} \right)^2 \approx \frac{1}{\left\langle h \right\rangle \left\langle n_{0-PAG} \right\rangle} \left[1 - \frac{\left(1 - \left\langle h \right\rangle\right)^2 \ln\left(1 - \left\langle h \right\rangle\right)}{\left\langle h \right\rangle} \left(\frac{Y_0}{\phi_e} \right) \right] \tag{29}$$

It is instructive to compare the magnitudes of the two terms on the right-hand side of equation (24). For the sake of clarity of discussion, we shall define

$$\begin{aligned} Ideal\ acid\ shot\ noise &= \sqrt{\frac{1}{\left\langle h \right\rangle \left\langle n_{0-PAG} \right\rangle}} \\ Photoelectron\ shot\ noise &= \left| \frac{\left(1 - \left\langle h \right\rangle\right) \ln\left(1 - \left\langle h \right\rangle\right)}{\left\langle h \right\rangle} \right| \sqrt{\frac{1}{\left\langle n_{photoelectrons} \right\rangle}} \end{aligned} \tag{30}$$

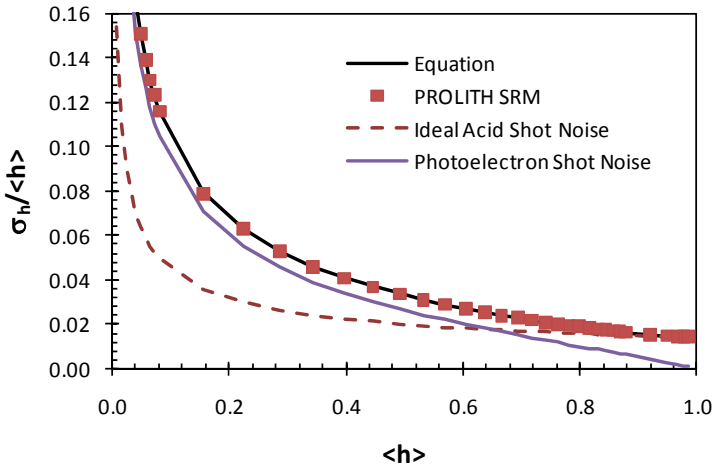

Figure 13. For the nominal parameters of Table II, the relative acid uncertainty along with the two components of uncertainty, as defined in equation (30).

The relative acid uncertainty, $\sigma_h / \langle h \rangle$, is the square root of the sum of the squares of these two terms. As Figure 13 shows for the nominal case of Table II, the Poisson acid shot noise dominates when $\langle h \rangle > 0.65$, and is limited by the initial PAG Poisson concentration uncertainty as $\langle h \rangle \to 1$. When $\langle h \rangle < 0.65$, the photoelectron term (which includes photon shot noise) dominates. The cross-over value of $\langle h \rangle$ (the value that makes the acid and photoelectron shot noise terms equal) is a function the initial acid yield, varying approximately as

$$\langle h \rangle_{crossover} \approx \frac{3}{4}\left(1 - \frac{\phi_e}{Y_0}\right) \tag{31}$$

V. DISCUSSION OF RESULTS

To model the mechanism of line-edge roughness formation in EUV resist, it is necessary to predict both the mean and the standard deviation of the acid concentration resulting from exposure. The PROLITH Stochastic Resist Model is a very valuable tool for making such predictions, for both the open-frame exposure test case employed in this work and the more general case of full EUV imaging. Additionally, this paper has proposed and validated analytical equations to predict mean and standard deviation of the acid concentration by matching to the PROLITH SRM. The advantage of the analytical expressions is their compactness and the intuitive way in which they point to optimization.

Consider the following important optimization question: given a certain exposure dose and a certain resist thickness, what can be done to reduce the relative uncertainty in the resulting acid concentration at the end of exposure? From equation (24), the options are limited:

- Increase the value of *C*, thus increasing $\langle h \rangle$
- Increase α (which increases *C* and thus $\langle h \rangle$, but also increases $\langle n_{photoelectrons} \rangle$)
- Increase ϕ_e (which increases both $\langle h \rangle$ and $\langle n_{photoelectrons} \rangle$)
- Increase the PAG loading, $\langle n_{0-PAG} \rangle$

These are the only approaches for reducing the relative acid concentration uncertainty for an EUV resist with a photoelectron exposure mechanism of the type modeled here. Of course, equation (14) details how each of the individual EUV resist parameters affect the value of the exposure rate constant *C*. Translating these modeling parameter goals into resist formulations, however, is challenging. The analytical expressions for *C* [equations (14) or (21)] and for the relative acid uncertainty $\sigma_h / \langle h \rangle$ [equation (24)] provide quantitative predictions of how much improvement will result from a given change in one of the relevant parameters.

The state-of-the-art in EUV resist design today is based on chemically-amplified systems with polymer-bound-PAGs.[8,9,10,11,12] These resists are capable of 22-nm half-pitch resolution with LWR of 4.2 nm using a sizing dose of 11 mJ/cm^2 and a 0.30 NA, dipole illumination exposure tool. At the expected dose requirements of no more than 15 mJ/cm^2, LWR remains the most difficult challenge, especially when coupled with continued reductions in feature size. However, based in part on our understanding of the EUV reaction mechanism discussed here, we can improve EUV resists using several approaches:

- Increase resist absorption of EUV light

- Reduce the electron affinity of the matrix polymer
- Increase the electron affinity of the PAG
- Minimize electron blur by increasing resist atomic density
- Minimize acid diffusivity by using lower activation energy leaving groups and reduced post-exposure bake temperatures
- Reduce the spatial distribution fluctuations of PAG in the resist
- Reduce resist sensitivity to out-of-band radiation

EUV resist development is still at an early stage. Due to the photospeed constraints placed on EUV resists, a non-chemically amplified resist approach is not practical. Fortunately, there are a number of unique resist levers arising out of the EUV reaction mechanism which provide opportunity to improve EUV chemically amplified resists.

VI. CONCLUSIONS

When based on accurate statistical-mechanical models, Monte Carlo approaches to simulating the stochastic nature of photoresist exposure (such as the PROLITH SRM) are extremely valuable. Such simulators are also an invaluable tool to help find simple, analytical formulas that can describe the basic stochastic behavior of resists. For 193-nm and related resists, the mechanism of exposure is simple enough that such analytical formulas can be derived from first principles. For EUV resists, with their complicated photoelectron and secondary electron exposure mechanism, a rigorous first-principles solution seems out of reach. However, by combining these two powerful tools (analytical and Monte Carlo approaches) important insights into the stochastic nature of EUV exposure can be obtained.

A method of finding the exposure rate constant C from a stochastic simulator has been demonstrated and its accuracy validated. The EUV exposure mechanism used by the PROLITH SRM was shown to be first order (as expected). Further, the influence of each PROLITH SRM parameter on C has been detailed to the point where a simple, semi-empirical expression predicts C to within about 1%. With this expression, one can conveniently predict the mean concentration of acid as a function of exposure dose. This prediction is important since the mean acid concentration is needed to predict the standard deviation of the acid concentration.

For line-edge roughness modeling, predicting the standard deviation of the acid concentration at the end of exposure is an important first step. Extensive PROLITH SRM simulations have shown that a simple and intuitive analytical expression can predict the relative standard deviation of the acid concentration quite accurately. A main advantage of this expression, besides its usefulness in an overall model for LER, is to gain insight into what resist formulation and processing changes might improve the acid concentration uncertainty, and what the magnitude of the improvement will be. Further, this analytical model can provide a practical guideline for predicting a limit for how low LER can be made, within the paradigm of the current EUV resist exposure mechanism. A summary of the final model equations are shown below.

$$C = d_e \alpha \phi_e \phi_{PAG} \sigma_{e-PAG} \left(\frac{\lambda}{hc} \right)$$

$$d_e = d_0 \left(1 - \frac{IP}{110eV} \right)$$

$$\sigma_{e-PAG} = \pi (r - r_o)^2 \qquad r_o = 0.0084 E_{excit}^2$$

$$\frac{\sigma_h^2}{\langle h \rangle^2} = \frac{1}{\langle h \rangle \langle n_{0-PAG} \rangle} + \left(\frac{\left(1 - \langle h \rangle\right) \ln\left(1 - \langle h \rangle\right)}{\langle h \rangle} \right)^2 \frac{1}{\langle n_{photoelectrons} \rangle}$$

$$\langle n_{photoelectrons} \rangle = \phi_e \langle n_{photons} \rangle \left(1 - e^{-\alpha D}\right) \qquad \langle h \rangle = 1 - e^{-C\langle E \rangle}$$

APPENDIX

Consider the open-frame exposure of a thin layer of (non-bleaching) photoresist on a non-reflective substrate. The acid concentration h resulting from exposure, for a first-order exposure mechanism, will be

$$h(z) = 1 - e^{-CE(z)} \tag{A.1}$$

where C is the exposure rate constant (Dill exposure parameter), z is the depth into the resist, and the depth dependence of the exposure dose E is due only to absorption:

$$E(z) = E_i e^{-\alpha z} \tag{A.2}$$

where α is the resist absorption coefficient and E_i is the dose at the top of the resist. For these simulations, an immersion fluid is used with the same refractive index (real part) as the resist so that there is almost no reflections at the fluid-resist interface and E_i is essentially the incident dose.

For stochastic simulations, one cannot determine $h(z)$ at an arbitrary z value, only an average value of h can be determined over a range of thickness for any given simulation. Averaging over the thickness of the resist D,

$$h_{AVG} = 1 - \frac{1}{D}\int_0^D e^{-CE(z)} dz \tag{A.3}$$

In anticipation of needing Taylor series expansions to derive a useful solution to equation (A.3), let us break up the exposure dose as a function of depth into the resist into an average dose E_{AVG} and a deviation from this average, $\Delta(z)$:

$$E(z) = E_{AVG} + \Delta(z) \tag{A.4}$$

where

$$E_{AVG} = \frac{1}{D}\int_0^D E_i e^{-\alpha z} dz = E_i\left(\frac{1 - e^{-\alpha D}}{\alpha D}\right) \tag{A.5}$$

Thus,

$$\Delta(z) = E_i\left(e^{-\alpha z} - \frac{1 - e^{-\alpha D}}{\alpha D}\right) \tag{A.6}$$

Combining equations (A.3) and (A.4),

$$1 - h_{AVG} = e^{-CE_{AVG}} \frac{1}{D}\int_0^D e^{-C\Delta(z)} dz \tag{A.7}$$

Taking the log of both sides,

$$-\ln(1-h_{AVG}) = CE_{AVG} - \ln(\delta) \quad where \quad \delta = \frac{1}{D}\int_0^D e^{-C\Delta(z)}dz \tag{A.8}$$

For a thin resist (αD « 1) we expect $C\Delta(z)$ « 1 and $\delta \sim 1$. If $\ln(\delta)$ can be neglected, a plot of $-\ln(1-h_{AVG})$ versus E_{AVG} will give a straight line with slope equal to C.

To determine the error in using a straight-line fit to find C, we will evaluate equation (A.8) for δ by using a Taylor expansion of the exponential out to second-order terms:

$$e^{-C\Delta(z)} \approx 1 - C\Delta(z) + \frac{(C\Delta(z))^2}{2} \tag{A.9}$$

For this expansion, δ becomes

$$\delta \approx 1 - \frac{1}{D}\int_0^D C\Delta(z)dz + \frac{C^2}{2D}\int_0^D \Delta^2(z)dz \tag{A.10}$$

The first integral on the right-hand side of equation (A.10) will be zero since the definition of $\Delta(z)$ requires it to have an average value of 0. Substituting equation (A.6) into equation (A.10) and carrying out the integration,

$$\delta \approx 1 + \frac{1}{2}(CE_i)^2\left(\frac{1-e^{-2\alpha D}}{2\alpha D} - \left[\frac{1-e^{-\alpha D}}{\alpha D}\right]^2\right) \tag{A.11}$$

Again using a Taylor expansion of the exponentials and keeping only terms to $O([\alpha D]^2)$,

$$\delta \approx 1 + \frac{1}{24}(\alpha D C E_i)^2 \tag{A.12}$$

Putting this result into equation (A.8) and using a Taylor expansion of the logarithm to the same order,

$$-\ln(1-h_{AVG}) \approx CE_{AVG} - \frac{1}{24}(\alpha D C E_i)^2 \tag{A.13}$$

Fitting data represented by equation (A.13) to a straight line will produce an error in determining C proportional to the quadratic term in equation (A.13). For this work, the range of exposure energies used for this fit was chosen so that CE_i was in the range from 0 to about 2.5 – 3. Empirically, it was observed that the straightly line fit passed through the quadratic curve at about 80% of the maximum dose. Thus, the straight-line fit value of C, C_{fit}, was smaller than the actual value of C by about

$$C_{fit} \approx C\left(1 - \frac{(\alpha D)^2}{12}\right) \tag{A.14}$$

To determine if this error is significant (and thus whether the straight-line fit is an appropriate method for determining C from a set of stochastic simulations), we compare the systematic error predicted by equation (A.14) to the random error that results from stochastic simulations. For 193-nm resist simulations, we have the added advantage of knowing the true value of C for the simulations. The 193-nm test case used the parameters found in Table I. To determine the random uncertainty in the measured C due to stochastic effects, the straight-line fit value of C was determined 20 times under identical circumstances (changing only the random seed for the simulations) and the standard deviation of the values calculated. The results are shown in Table IV (along with the 95% confidence interval for the sample standard deviation). Roughly, the uncertainty in C decreases as the reciprocal of the square root of the number of trials and as the reciprocal of the square root of the resist thickness.

Table IV. Standard deviation of C from 20 repeated simulation experiments for each 193-nm test case.

	100 trials per dose	1000 trials per dose
D = 10 nm	0.045 ± 0.014%	0.015 ± 0.005%
D = 50 nm	0.027 ± 0.009%	0.0057 ± 0.0018%

Setting the systematic error predicted by equation (14) equal to the random error estimated based on Table IV, the maximum resist thickness for which the straight-line approach is reasonable can be estimated. Of course, one could always fit the simulated data to the second-order model of equation (A.13), producing reasonable results even for much thicker resists. The purpose of using the straight-line fit approach is for the convenience of the data analysis only. For an EUV resist with D = 10 nm, α = 6.5 μm^{-1} (plus the EUV test case parameters from Table II) and using 100 trails per exposure dose, the standard deviation in determining C is about 0.036% ± 0.009%. This is about equal to the systematic error in using the linear approach for measuring C, $(\alpha D)^2/12$, so that 10 nm is about the limit for how thick such an EUV resist can be when applying the linear method for extracting C.

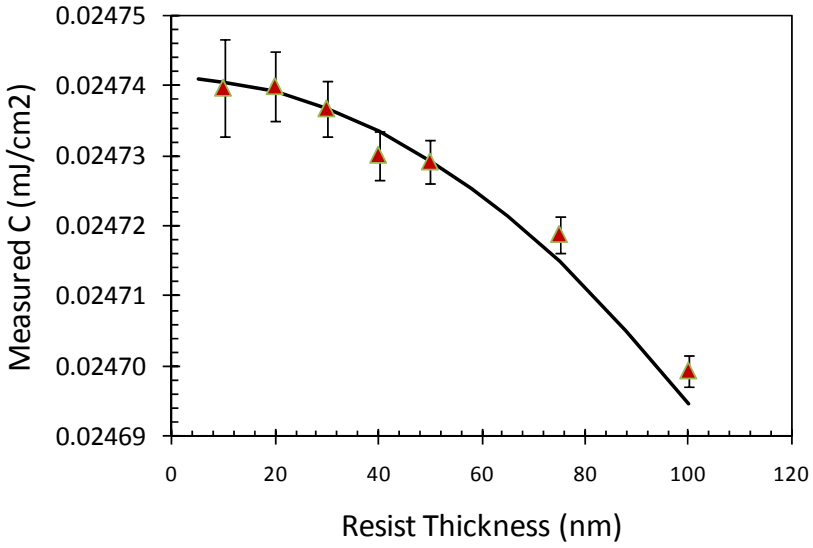

Figure 14. Using a straight-line fit, the measured value of C (data points) as a function of resist thickness for the simulation conditions of Table I (1000 trials per dose). The solid line shows the expected value using equation (A.14).

---

[1] T. Kozawa and S. Tagawa, "Radiation Chemistry in Chemically Amplified Resists", *Japanese Journal of Applied Physics*, 49, p 030001 (2010).

[2] F. H. Dill, W. P. Hornberger, P. S. Hauge, and J. M. Shaw, "Characterization of Positive Photoresist," *IEEE Trans. Electron Devices*, 22 (7), pp. 445-452 (July, 1975).

[3] C. A. Mack, "Absorption and Exposure in Positive Photoresist," *Applied Optics*, 27 (23), pp. 4913-4919 (1 Dec. 1988).

[4] J. Biafore, M. Smith, E. Setten, T. Wallow, P. Naulleau, D. Blankenship, S. Robertson, Y. Deng, "Resist pattern prediction at EUV", *Proc. SPIE,* 7636, p. 76360R-1 (2010).

[5] Chris A. Mack, Fundamental Principles of Optical Lithography: The Science of Microfabrication, J. Wiley & Sons (London, 2007), p. 195-197.

[6] Chris A. Mack, Fundamental Principles of Optical Lithography: The Science of Microfabrication, J. Wiley & Sons (London, 2007), p. 245. An error in the first and second printing of this book gives a slightly incorrect version of equation (6.70) on page 245. The error is corrected when the equation is reproduced in this paper.

[7] Chris Mack, "A Simple Model of Line-Edge Roughness", *Future Fab International*, Vol. 34 (July 14, 2010).

[8] James W. Thackeray, Roger A. Nassar, Robert Brainard, Dario Goldfarb, Thomas Wallow, Yayi Wei, Jeff Mackey, Patrick Naulleau, Bill Pierson, and Harun H. Solak, "Chemically amplified resists resolving 25 nm 1:1 line-space features with EUV lithography", *Proc. SPIE*, 6517, p. 651719 (2007).

[9] J. W. Thackeray, R. A. Nassar, K. Spear-Alfonso, R. Brainard, D. Goldfarb, T. Wallow, Y. Wei, W. Montgomery, K. Petrillo, O. Wood, C.–S. Koay, J. Mackey, P. Naulleau, B. Pierson, H. Solak, "Pathway to sub-30 nm Resolution in EUV Lithography", *J. Photopolym. Sci. Tech*., 20 (3), pp. 411-418 (2007).

[10] M. Thiyagarajan, K. Dean, K. Gonsalves, "Improved Lithographic Performance for EUV resists based on Polymers with Photoacid Generators in the Backbone", *J. Photopolym. Sci Tech.*, 18 (6), pp. 737-741 (2005).

[11] Robert D. Allen, Phillip J. Brock, Young-Hye Na, Mark H. Sherwood, Hoa D. Truong, Gregory M. Wallraff, Masaki Fujiwara and Kazuhiko Maeda, "Investigation of Polymer-bound PAGs: Synthesis, Characterization and Initial Structure/Property Relationships of Anion-bound Resists", *J. Photopolym. Sci. Tech*., 22 (1), pp. 25-31 (2009).

[12] Joonhee Han, Jung Hoon Oh, Hyun Sang Joo, Hyun Soon Lim, Seung Duk Cho, Jin Bong Shin, So Jung Park, Dong Chul Seo, "Studies of Acid Diffusion of Anionic or Cationic Polymer Bound PAG", presented at *EUV Symposium 2010*, Chiba Japan (2010).